Chemical Geology 643 (2024) 121822

Contents lists available at ScienceDirect

Chemical Geology

journal homepage: www.elsevier.com/locate/chemgeo

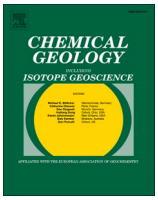

Active near-surface mobilisation of slab-derived geochemical signatures by hyperalkaline waters in brecciated serpentinites

Aled D. Evans [a,*], Dave Craw [b], Damon A.H. Teagle [a]

[a] School of Ocean and Earth Science, National Oceanography Centre Southampton, University of Southampton, Southampton SO14 3ZH, UK
[b] Department of Geology, University of Otago, P.O. Box 56, Dunedin, New Zealand

ARTICLE INFO

Editor: Michael Böttcher

Keywords:
Serpentinization
Serpentinite diapirism
Hyperalkaline waters
Fluid-rock interaction
Subduction zone
Meteoric water

ABSTRACT

Unusual hyperalkaline meteoric groundwaters on Troodos massif, Cyprus, issue from highly deformed and completely serpentinized ultramafic brecciated rock masses of the Artemis Diapir and have high salinity (25–30% seawater total dissolved solids) and some of the highest recorded pH values (11−13) for natural waters. These waters have elevated dissolved Na, K, Li, B, Ba, Rb, Cs, Cl and SO_4 with ion/chloride substantially above seawater ratios, overprinting minor contributions from marine aerosols. For example, K concentrations are similar to seawater values. Water stable isotope ratios imply extensive water-rock interaction and $^{87}Sr/^{86}Sr$ is rock-dominated (0.705) and significantly lower than seawater. These rare fluids contrast with surface and shallow ground waters draining the ultramafic Troodos Mantle Sequence that have pH of 8.5–9, meteoric stable isotope ratios, $^{87}Sr/^{86}Sr$ similar to early Miocene seawater (0.7085) and low dissolved salts albeit with ion/chloride ratios also greater than seawater. The combination of high pH and salinity is unusual in ophiolites and these hyperalkaline waters are most similar to end-member fluids emanating from serpentine mud volcanoes in the Mariana forearc. Rainwater rapidly transiting terraces of asbestos mine tailings on Troodos mostly resemble the surface waters but show slight contamination by a saline component. We propose that inclusions within the serpentinite that contain highly soluble salts have been made accessible by tectonic deformation during uplift and diapirism, or comminution during mining activity. A multistage process is proposed whereby alkali and other signatures have been released from the stalled subducting slab beneath the Troodos massif and have infused the mantle wedge. Some of these rocks have been carried to the surface by diapiric uplift and erosion, where tectonic deformation or mining activities have enabled the near-surface mobilisation of slab-derived geochemical signatures by modern meteoric waters.

1. Introduction

Interactions between water and mantle rocks, termed serpentinization, play critical roles in the Earth system (Kerrick, 2002). Hyperalkaline pH >11 waters associated with serpentinized peridotites, emanate from subaerial and submarine vents and commonly form terraces or chimneys composed of carbonates and brucite (Barnes et al., 1967; Barnes and O'Neil, 1969; Kelley et al., 2001). It is generally accepted that these fluids formed through active low temperature serpentinization reactions, but their genesis, evolution, and relationship to other water types in the same setting remains enigmatic.

Two contrasting primary water types are reported emanating from continental serpentinized massifs: (1) a meteoric-derived pH <10, surficial, primarily magnesium-bicarbonate water (often referred to as "Type 1" fluids); and (2) a hyperalkaline pH >10, meteoric-derived, primarily calcium-hydroxide water that is sourced from deeper within the hydrological system (e.g., Samail ophiolite, Oman; California, USA; Liguria, Italy; "Type 2" fluids of Barnes et al., 1978, 1967; Barnes and O'Neil, 1969; Boschetti et al., 2013; Chavagnac et al., 2013; Giampouras et al., 2019; Kelemen and Matter, 2008; Monnin et al., 2014). These hyperalkaline pH >10 waters are not limited to continental serpentinized massifs, but also occur in the off-axis low-temperature (~100°C) Lost City Hydrothermal Field atop the Atlantis Massif, Mid Atlantic Ridge (Kelley et al., 2001), in serpentine mud volcanoes in the Mariana Forearc (Mottl et al., 2004), and in Prony Bay, New Caledonia (Monnin et al., 2014).

Previous studies (e.g., Neal and Stanger, 1985) predict that once serpentinization of primary minerals is complete, hyperalkaline waters

* Corresponding author.
E-mail address: A.Evans@soton.ac.uk (A.D. Evans).

https://doi.org/10.1016/j.chemgeo.2023.121822
Received 12 September 2023; Received in revised form 2 November 2023; Accepted 7 November 2023
Available online 9 November 2023

will cease to form in completely serpentinized mantle rocks. However, high pH hyperalkaline waters are present in many systems where the outcrops of mantle peridotite are strongly to completely serpentinized and primary mantle minerals are only minor components (Kelemen et al., 2011; Saad, 1969).

Due to the abundance of partially serpentinized mantle peridotites atop the Troodos mountains, one might predict the common occurrence of high pH fluids hosted by the Mantle Sequences of the Troodos ophiolite, but hyperalkaline springs are rare and few have been comprehensively characterised (Neal and Shand, 2002; Rizoulis et al., 2016). Here, we report analyses of previously undocumented high pH springs and other groundwaters hosted by highly deformed completely serpentinized rocks from the Artemis Diapir (Evans et al., 2021) of the Troodos Mantle Sequence, Cyprus. We propose that these hyperalkaline waters are formed by reactions between modern meteoric-water and serpentine rather than active low-temperature serpentinization

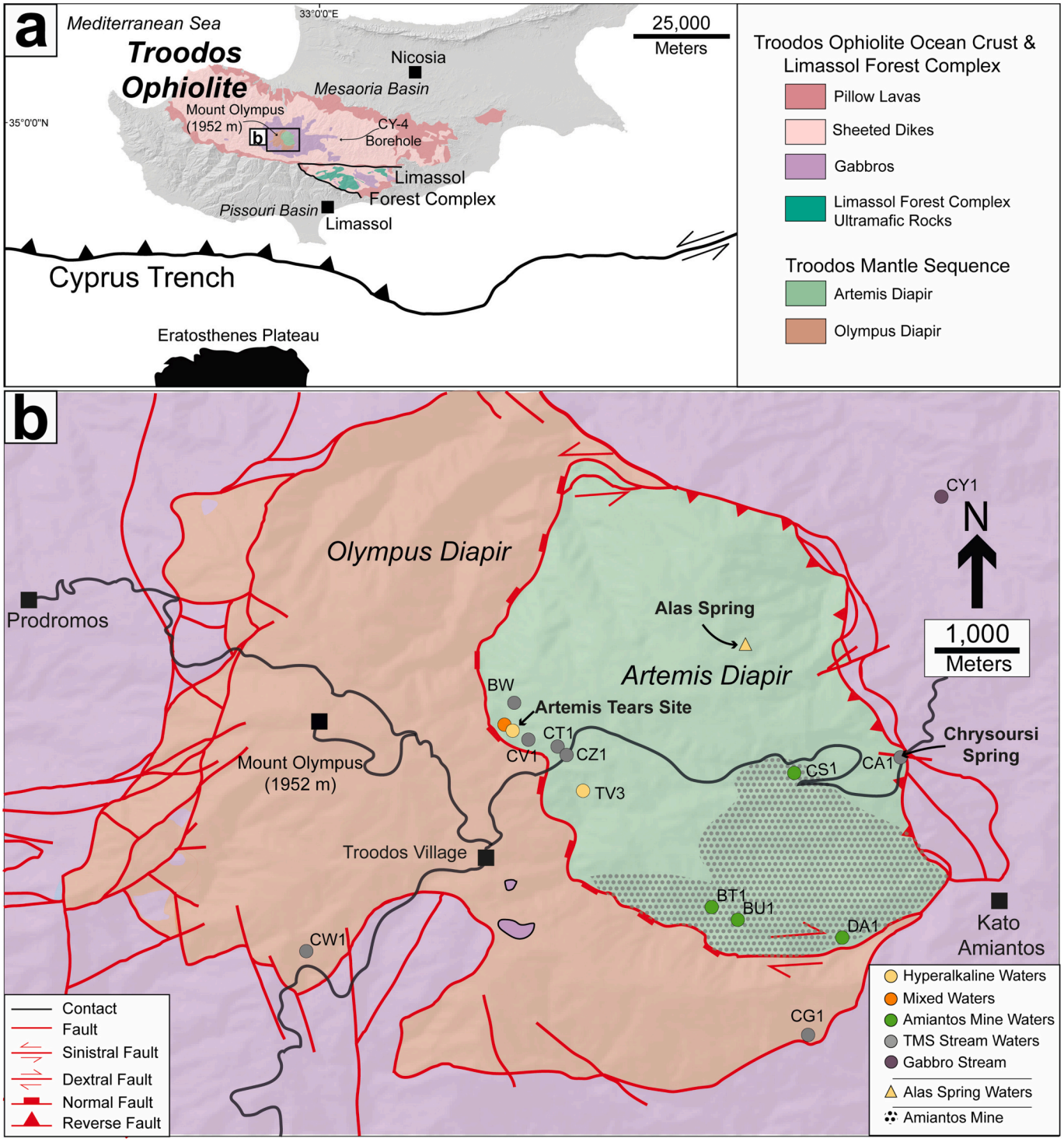

Fig. 1. (a) Locations of water samples and detailed geological map of the Troodos ophiolite with the bullseye geometry of the Mantle Sequence highlighted along with the Limassol Forest Complex, the Cyprus Trench, and northernmost extent of the Eratosthenes Plateau. (b) Geological map of the Troodos Mantle Sequence (updated from Wilson, 1959). Shaded area shows the abandoned Amiantos asbestos mine.

hydration reactions of primary mantle minerals. The unusual chemistry of these meteoric-derived high pH fluids ultimately reflects signatures of subducted materials that have been mechanically advected through the underlying Cyprus mantle wedge by serpentinite diapirism and subsequently mobilised by meteoric waters.

2. Geological setting of the Troodos Mantle Sequence

Serpentinized mantle rocks of the Troodos Mantle Sequence form the highest elevations of Cyprus (Mount Olympus, 1952 m asl). These strongly to completely serpentinized mantle peridotites are surrounded by an anticlinal dome comprising concentric annuli of gabbroic and ultramafic cumulate rocks, sheeted dikes, lavas, and submarine sediments that crop out at progressively lower elevations (Fig. 1). The Troodos ophiolite exposes ocean crust and upper mantle rocks that formed ~90–92 Ma at some form of supra-subduction zone spreading ridge in the Neotethyan Ocean (Moores et al., 1984; Moores and Vine, 1971; Mukasa and Ludden, 1987; Pearce et al., 1984). The Troodos Mantle Sequence has been sub-divided into two contrasting serpentinite diapirs (Evans et al., 2021; Gass and Masson-Smith, 1963; Moores and Vine, 1971; Wilson, 1959) that we refer to as (i) the Olympus Diapir, an arcuate domain of partially (~50 to 70%) serpentinized tectonized harzburgites with minor dunites that is juxtaposed by faults against (ii) the Artemis Diapir. Previously referred to as the "Smash Zone" (Wilson, 1959), the Artemis Diapir is a subcircular domain of friable, completely serpentinized mantle peridotite blocks in a sheared matrix of serpentine breccia and comminuted serpentine gouge and clasts formed by multiple generations of serpentine deformation and recrystallization (Fig. 1b; Evans et al., 2021). The Artemis Diapir includes the abandoned Amiantos asbestos mine (~100 Mt; Wilson, 1959). Deformed serpentinite muds and breccias dominate the periphery of Artemis Diapir and these steep outcrop slopes comprise friable matrixes of serpentine clay gouge and comminuted serpentine cataclasite that have undergone multiple episodes of deformation and recrystallisation (Evans et al., 2021).

The progressive uplift and unroofing history of the Troodos massif is preserved in circum-Troodos sedimentary sequences that indicate that significant subaerial uplift and exposure uplift was initiated ~5.5 Ma (McCallum, 1989; Morag et al., 2016; Poole and Robertson, 1991; Robertson, 1977; Rouchy et al., 2001; Stow et al., 1995). Troodos-derived diabase and lava clasts occur in latest Messinian / Early Pliocene (~5.5 Ma) strata indicating active sub-aerial erosion of the uppermost Troodos crust by this time (McCallum, 1989; Rouchy et al., 2001; Stow et al., 1995). This is in good agreement with low-temperature (U—Th)/He thermochronology on plutonic rocks from the Troodos Massif that suggests an exhumation rate of 0.86 mm/yr with the onset of uplift at 6 ± 2 Ma (Morag et al., 2016). The first occurrences of ultramafic clasts are within the Lower Pleistocene (<2.58 Ma) sequence (Poole and Robertson, 1998, 1991; Stow et al., 1995; Wilson, 1959) and the abundance of ultramafic clasts progressively increases within the Pleistocene Fanglomerate sequences (2.58–0.0117 Ma) (Poole and Robertson, 1998, 1991). The intensity of the uplift has waned from the Late Pleistocene to the present day (Poole and Robertson, 1998).

A major gravity low centred on the Artemis Diapir has been modelled as a deep ~11 km cylinder of low-density (2700 kg/m^3) material (Gass and Masson-Smith, 1963; Shelton, 1993). Trace element concentrations and contrasting chrome spinel compositions suggest that the Artemis Diapir serpentinites are from a different mantle region to the tectonized harzburgites of the Olympus Diapir that partially melted to form the crustal rocks of the Troodos ophiolite (Batanova and Sobolev, 2000).

3. Groundwaters of the Troodos ophiolite

Water is of fundamental importance to Cyprus due to its arid eastern Mediterranean climate. Run off from the Troodos mountains is essential for recharging the aquifers in the low-lying circum-Troodos sediments on time scales of decades (Boronina et al., 2005b, 2005a, 2003; Georgiou, 2002; Mederer, 2009). Mountain springs and boreholes hosted by Troodos crustal rocks provide potable water for drinking, bottling and local irrigation. Recent comprehensive investigations of groundwaters from the crustal section of the Troodos ophiolite (Christofi et al., 2020a, 2020b) has established the range of fluid types within these fractured reservoirs but did not characterise wells or springs hosted by the Troodos Mantle Sequence (elemental analyses of two springs emanating from or near the Troodos Mantle Sequence are presented in Christofi, 2020). Fluids from wells in gabbroic rocks that surround the mantle domain, albeit at lower altitudes, are generally fresh with low chlorinity and sodium concentrations less than Mg or Ca concentrations (MgCa-$NaHCO_3$ type fluids following Christofi et al., 2020a, 2020b). Na/Cl_{molar} ratios are elevated compared to modern seawater (x2.2 ± 0.9 1σ; n = 50). Hydrochemical modelling indicates that most fluids result from low temperature exchanges with host rock minerals, but a minority of samples indicate minor input (≤0.1%) of a formation water proposed to be seawater (Christofi et al., 2020a). Higher concentrations of Na, Cl and SO_4 are more common in waters from wells from the stratigraphically overlying dikes, basal group and lavas of the Troodos upper crust that surround the gabbros at progressively lower elevations (Christofi et al., 2020a, 2020b; Neal and Shand, 2002). The lavas are overlain by Cretaceous to modern Circum-Troodos sedimentary sequences that irregularly include Messinian evaporite sequences that developed in small semi-isolated basins (Manzi et al., 2016; Rouchy et al., 2001; Stow et al., 1995). Investigations of cores from Cyprus Crustal Study Project Hole CY-2A drilled into mineralised lavas identified gypsum and trace amounts of anhydrite that yield $\delta^{34}S$ values ranging between +21.8 and +22.7 ‰ (Alt, 1994; Herzig and Friedrich, 1987; Jamieson and Lyndon, 1987). These open space-filled sulfate minerals are proposed to have formed from groundwaters circulating within the Troodos lavas that remobilised sulfate from the overlying Messinian evaporite sequences. However, there is only trace sulfate in rocks from Hole CY-4 that drilled the >2000 m through the lowermost sheeted dikes, into gabbros and cumulate ultramafic rocks, indicating that this Messinian signature is absent or only poorly developed in the plutonic sections of the Troodos crust (Alt, 1994).

Here we present new major and trace element concentrations and Sr and stable isotope analyses (O, H) of surface and groundwaters from the Mantle Sequences of the Troodos ophiolite with emphasis on rare hyperalkaline (pH >11) seeps (Table 1, Fig. 1b). Samples were collected from streams, springs, seeps and snow from both the Olympus and Artemis domains of the Troodos Mantle Sequence (Table S1). An additional sample set was collected from streams, seeps and lake draining recently groomed and partially afforested tailings terraces of the Amiantos asbestos mine. Analysis of stream water from a gabbro-only catchment complements published data (Christofi et al., 2020b; Neal and Shand, 2002). Details of analytical methods are recorded in Supplementary methods.

3.1. Groundwaters from the Troodos Mantle Sequences

The dominant waters flowing in streams and springs hosted by the Troodos Mantle Sequences are fresh, Mg-bicarbonate fluids with pH between 8.1 and 9.6 (Fig. 2a). These Troodos Mantle Sequence surface (TMS) waters are similar to gabbro-hosted groundwaters (Christofi et al., 2020a), but with generally higher pH and Mg (x3) but are fresher with relatively low Cl, Na, Ca, and sulfate concentrations (Table 1). The latter two parameters are lower by an order of magnitude although Ca is relatively less depleted than sulfate compared to seawater. TMS waters are the equivalent of Type 1A and 1B Cyprus fluids of Neal and Shand (2002) and are similar to other Mg-HCO_3 "Type 1" surface fluids reported from the mantle sequences of numerous ophiolites (e.g., Barnes and O'Neil, 1969; Chavagnac et al., 2013; Leong et al., 2021). Most TMS waters have Na/Cl less than modern seawater, but elevated K, Rb and Cs

Table 1
Composition of waters from the Troodos Mantle Sequence and comparison fluids. Bold emphasises concentrations greater than modern seawater. † Data sourced from Mottl et al. (2004).

Type	Troodos Mantle Sequence surface waters (TMS-waters)	Artemis hyperalkaline waters	Amintos Mine waters	Modern seawater	Mariana Serpentine Springs†
Diapir	Olympus & Artemis	Artemis	Artemis		
n	10	9	4		3
pH	8.2 to 9.6	11.5 to 13.0	8.5 to 9.0	8.15	11.42 to 12.5
Salinity g/kg	0.16 to 0.28 fresh	5.4 to 15.0 brackish	0.28 to 0.72 fresh to weakly brackish	34.5 saline	24.1 to 36.6 brackish to saline
Water classification	$MgHCO_3$ > $MgHCO_3CO_3$	NaCl to NaClOH	$MgNaHCO_3Cl$ > $MgHCO_3$	NaCl	NaCl > $NaClSO_4$
T °C	10.4 to 19.8	9.0 to 22.2	13.5 to 16.3		
$^{87}Sr/^{86}Sr$	0.7084 to 0.7086	0.7056 to 0.7059	0.7079 to 0.7086	0.70918	0.7054 to 0.7063
$\delta^{18}O$ (per mil, VSMOW)	−7.6 to −6.6	−5.4 to −3.0	−7.0 to −7.1	0	2.5 to 4.0
δD (per mil, VSMOW)	−39 to −33	−33 to −29	−37 to −35	0	−4.8 to 14.2
Cl mmol/kg	0.32 to 0.40	**77 to 222**	0.9 to 6.4	546	**260 to 518**
SO_4	0.03 to 0.05	1.7 to 5.2	0.06 to 0.15	27.2	**27 to 46**
DIC	4.1 to 8.1	0.6 to 3.8	6.2 to 10.1	1.97	9 to 29
Mg	2.6 to 4.5	0.008 to 2.3	3.9 to 6.6	52.8	b.d. to 0.003
Ca	0.03 to 0.23	0.16 to 0.95	0.11 to 0.16	10.3	0.3 to 1
Na	0.21 to 0.41	**100 to 273**	1.0 to 5.8	465	**390 to 610**
K	0.006 to 0.02	**3.3 to 8.1**	0.03 to 0.25	10.2	**15 to 19**
B (μmol/kg)	9 to 70	**657 to 3134**	40 to 100	415	**3200 to 3900**
Li	0.6 to 3.8	**730 to 2417**	9.5 to 25.5	25.6	0.02 to 1.6
Rb	0.002 to 0.01	**2.2 to 5.3**	0.025 to 0.42	1.45	**7.8 to 10**
Cs	0.025 to b.d.	**0.5 to 1.9**	0.02 to **0.68**	0.002	**0.15 to 0.36**
Sr	0.03 to 0.3	0.2 to 1.1	0.14 to 0.24	90.7	10 to 20
Ba	0.0004 to 0.03	0.08 to **0.18**	0.08 to **0.37**	0.085	0.1 to **0.4**
Si	5 to 816	34 to 312	150 to 383	110	24 to 70
Br	b.d. to 52	b.d. to 239	8.6 to 97	842.1	n.a.
Na/Cl (mol/mol)	0.63 to **1.0**	**1.20 to 1.35**	0.91 to **1.12**	0.85	**1.1 to 1.5**

over Cl ratios compared to modern seawater albeit at much lower concentrations. Similarly, B and Li are present in only low concentrations although they are strongly enriched compared to Cl relative to seawater. B/Li ratios are ~15 to 23 (Fig. 2b), similar to or slightly elevated from modern seawater. In contrast, Sr is depleted relative to Ca compared to seawater. The Sr isotopic compositions of TMS waters are tightly clustered with $^{87}Sr/^{86}Sr = 0.7085 \pm 0.0001$ (1σ, $n = 6$) significantly higher than the range estimated for the mantle domain that sourced the magmas that formed the Troodos crust (0.7035–0.7039, Rautenschlein et al., 1985) and ~ 91 Ma seawater (~0.7073, McArthur et al., 2012). The Sr-isotopic compositions of TMS waters are of 18.5 to 21.5 Ma (Fig. 3a) seawater but within the range of ratios measured for Messinian evaporite sequences in the eastern Mediterranean (e.g., Schildgen et al., 2014). Oxygen and hydrogen stable isotope composition measurements of the TMS waters plot close to the local meteoric water line for the Troodos mountains (Fig. 3c, Boronina et al., 2005a; Christofi et al., 2020b).

3.2. Occurrences of hyperalkaline springs and Artemis hyperalkaline waters

The hyperalkaline springs documented in our study are hosted by highly deformed completely serpentinized rocks that crop out towards the base of the steep-sided valleys that delineate the boundary between the Artemis and Olympus domains (Fig. 4). These outcrops comprise friable mixtures of clay-sized serpentine gouge and comminuted serpentine cataclasite. In this boundary zone rare, small (<15 cm-wide) fluid seeps emanate from the serpentine breccias indicated by small zones of pyroaurite ($Mg_6Fe_2^{3+}(OH)_{16}[CO_3].4H_2O$) brucite, calcite and halite surface coatings. For example, a series of small ~3 m-wide travertine sites occur along the southern extent of this contact (TV3; Fig. 1b; Fig. 4a), where high pH >11 hyperalkaline waters emanate from serpentinite breccia and partially erode previously precipitated travertine deposits, forming small ~1 m-wide pools.

The best example of hyperalkaline fluid egress is the ~25 m-long Artemis Tears spring on the western boundary of the Artemis Diapir (Fig. 1b; Fig. 4b). Here, 9–17 °C hyperalkaline waters slowly emanate (~7 L/h) from a cluster of discrete springs along the break in slope near the valley floor. These discharges are surrounded by hard grounds of clastic surficial serpentinite grit cemented by calcite, aragonite, brucite, and halite. Along the surface drainage path of these hyperalkaline waters, soft, tacky, brucite-rich precipitates with minor carbonate, halite, and detrital serpentine have formed by mixing with other surface waters (Fig. 4b).

In contrast to TMS waters, these Artemis hyperalkaline waters are brackish (TDS 5 to 15 g/kg) with pH from 11.5 to 13 (Table 1; Fig. 2a). These fluids are mostly NaCl-type although hydroxide is a significant component of the pH ~13 fluids. Na/Cl ratios are elevated compared to seawater (1.2–1.3). Other ions provide only low contributions of the positive (Ca <0.7%; Mg <4%) or negative charge DIC <8.3%; SO_4 <2%). DIC concentrations are similar to or lower than TMS waters whereas SO_4 is increased by approximately a factor of 100, similar to Cl and Na (Fig. 5). Mg concentrations are lower than TMS waters but Ca and Sr concentrations are the same or slightly higher. Sr/Ca ratios show a similar range. SO_4 concentrations are approximately five times Ca. Ba concentrations are 10 to 100 times higher in the hyperalkaline fluids than the TMS waters. B concentrations are strongly elevated compared to TMS waters with concentrations up to seven times that of seawater. Li concentrations are even more strongly elevated, enriched by factors of 500 to >1000. Similarly, K, Rb and Cs concentrations are enriched by factors of 100 to ~1000 compared to TMS waters (Fig. 5). $^{87}Sr/^{86}Sr$ measurements yield surprisingly low ratios between 0.7056 and 0.7059, intermediate between estimated Troodos mantle and 91 Ma seawater (Fig. 3a,b) (McArthur et al., 2012; Rautenschlein et al., 1985). Oxygen

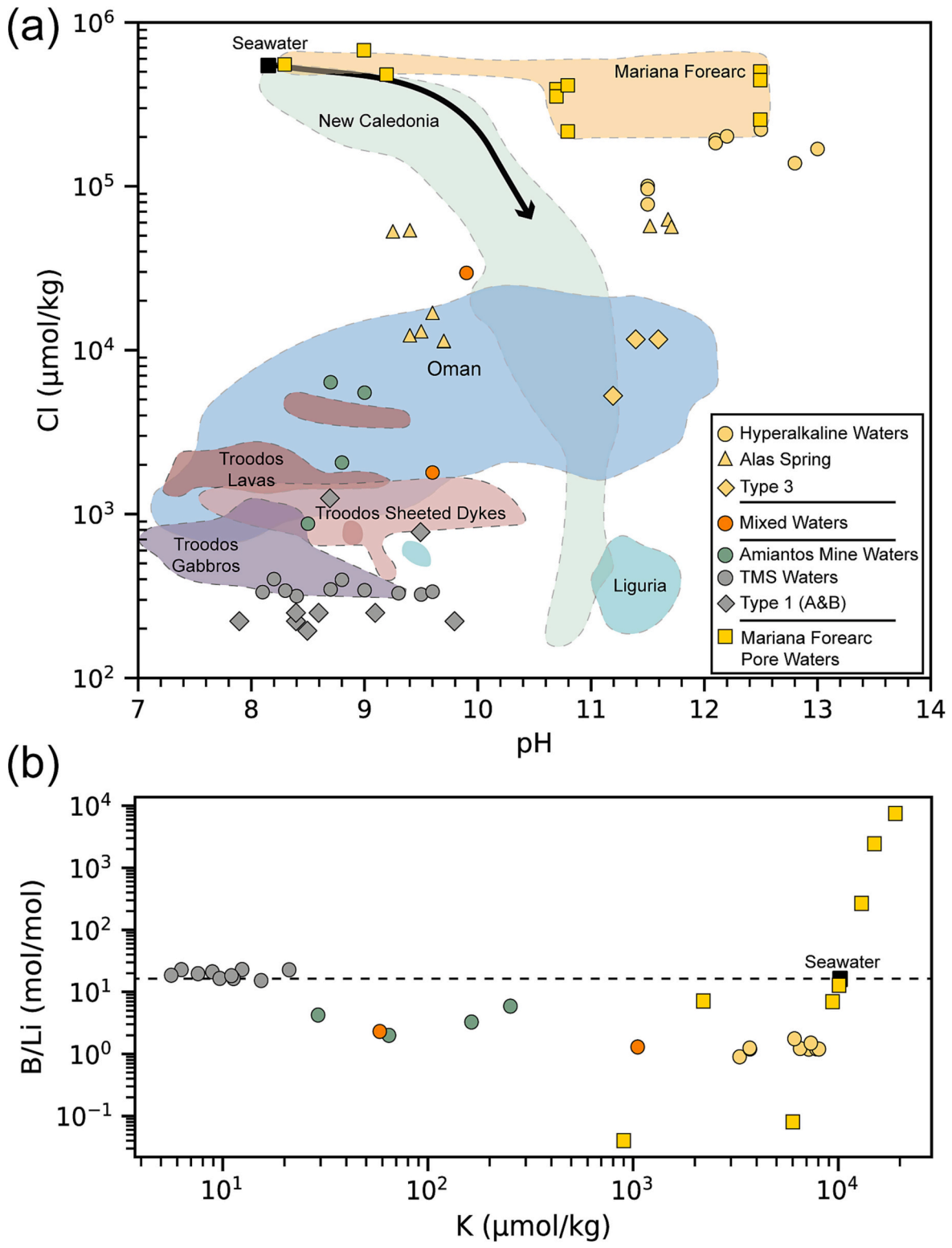

Fig. 2. (a) Cl versus pH data of waters sampled from the Troodos ophiolite. Alas spring samples are from Rizoulis et al. (2016) and Christofi (2020). Type 3 and Type 1 (A&B) waters from Neal and Shand (2002). New Caledonia (Monnin et al., 2014), Liguria (Chavagnac et al., 2013), Oman (Chavagnac et al., 2013; Leong et al., 2021), Troodos (Christofi et al., 2020a, 2020b; Neal and Shand, 2002) and the Mariana Forearc serpentinite mud volcanoes pore waters and springs (Hulme et al., 2010; Mottl et al., 2004; Wheat et al., 2018) are shown as fields. (b) B/Li (mol/mol) versus K concentration for Troodos fluids. Comparison data from Mariana forearc serpentinite waters. Dashed line shows seawater B/Li (mol/mol) ratio.

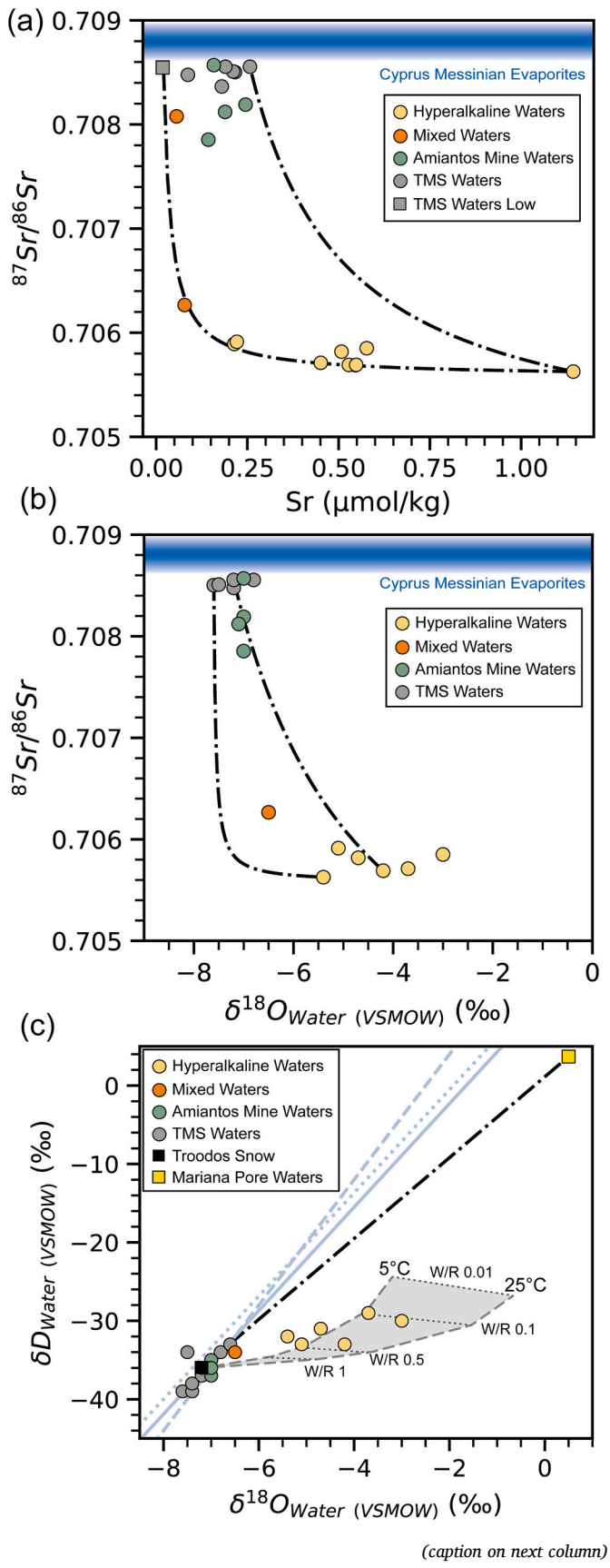

(caption on next column)

Fig. 3. (a) $^{87}Sr/^{86}Sr$ versus Sr and (b) $^{87}Sr/^{86}Sr$ versus $\delta^{18}O_{Water}$ plot of the Troodos Mantle Sequence waters. Dash-dotted black lines = mixing line. $^{87}Sr/^{86}Sr$ of Cyprus Messinian evaporites shown as a blue field (Schildgen et al., 2014). (c) $\delta^{18}O_{Water}$ versus δD_{Water} plot of Troodos Mantle Sequence waters. Dashed blue line refers to the Mediterranean meteoric water line (Gat et al., 1969), dotted blue line refers to the local Cyprus meteoric water line (Christofi et al., 2020a), solid blue line also refers to the local Cyprus meteoric water line (Boronina et al., 2005a). Gold squares shows the median Mariana Forearc Conical Seamount Pore Water (Benton, 1997) with a mixing line denoted as a black dash-dotted line with Troodos meteoric water. Light grey shaded area show a closed system water-rock (W/R) equilibrium model (Taylor, 1977) showing equilibrium at decreasing W/R ratios. Serpentine-water oxygen fractionation equations following (Wenner and Taylor, 1971) and hydrogen fractionation following (Saccocia et al., 2009).

and hydrogen stable isotopes also reveal rock-dominated signatures and are strongly shifted from the local meteoric water-line indicating exchange with serpentine at low water/rock ratios (w/r < 0.1; Fig. 3c).

Previously reported high pH fluids from the Troodos massif are similar to the hyperalkaline waters presented here, albeit with some differences. Earlier, reconnaissance sampling identified emissions of weakly to mildly brackish high pH fluids (pH 11.2 to 11.6) originating from the Troodos Mantle Sequences but issuing from gabbro-hosted wells (Types 3A; see Table S1; Neal and Shand, 2002) and have mixed with Ca, carbonate and sulfate-bearing groundwaters. Following Christofis et al., 2020a, these fluids are $NaClSO_4CO_3$ and $NaClCO_3$ waters and are not pure end-members. Sulfate is only rarely a major component of gabbro-hosted groundwaters (Christofi et al., 2020a) but is more common in the sheeted dikes and lavas. Unfortunately, the exact location of these wells is not reported. More recently, a microbiological study analysed high pH (9.3 to 11.7) mildly brackish NaCl-type fluids emanating from the Alas Spring that issues from a block of serpentinized peridotite cropping out on the north-eastern slopes of the Artemis Diapir (Fig. 1b, Rizoulis et al., 2016; see Table S1). These high pH Alas Spring fluids are essentially similar to our hyperalkaline fluids but are less saline and have very low Mg concentrations (Fig. 5) (Rizoulis et al., 2016). Complete alkali metal analyses are not available for the Alas Spring waters nor are Li and B concentrations, but high potassium concentrations, strongly elevated >100 times compared to TMS waters indicates similar alkali element enrichments.

The chemistry of the Artemis hyperalkaline waters are different from high pH fluids issuing from other peridotite massifs such as the Samail ophiolite, Oman (Fig. 2a). Sampled waters (pH from Samail ophiolite high pH waters (8.2 to 11.6) have relatively low alkali element concentrations Li, Na, K (Chavagnac et al., 2013; Leong et al., 2021). Importantly, oxygen and hydrogen stable isotopes of Oman hyperalkaline waters mostly fall on the local meteoric water line (e.g., Neal and Stanger, 1985) and do not display rock-dominated ratios like the Artemis hyperalkaline waters. Similarly, high pH >10.5 fluids hosted by peridotites in New Caledonia and Liguria have low chlorinities (Fig. 2a) (Chavagnac et al., 2013; Monnin et al., 2014). The saline, non-radiogenic $^{87}Sr/^{86}Sr$ Artemis hyperalkaline waters are strikingly similar to the end-member high pH waters emanating from serpentine mud-volcanoes in the Mariana forearc (Table 1; Figs. 2; 5; Hulme et al., 2010; Mottl et al., 2004).

3.3. Waters draining the Amiantos Asbestos Mine tailings

A selection of fluids were collected from streams, seeps and a small lake draining terraces of the ~130 Mt of tailings from the Amiantos Asbestos mine that operated from 1904 until 1988 (Fig. 1b). Although some terraces have been systematically replanted, there remain large, exposed banks of bare porous gritty mine waste. The mine waters are similar to TMS waters with pH between 8.5 and 9 but Cl, Na, Ba, Li and K concentrations are all elevated by approximately a factor of ten (Table 1, Fig. 2). Rb and Cs concentrations are even more strongly enriched. These

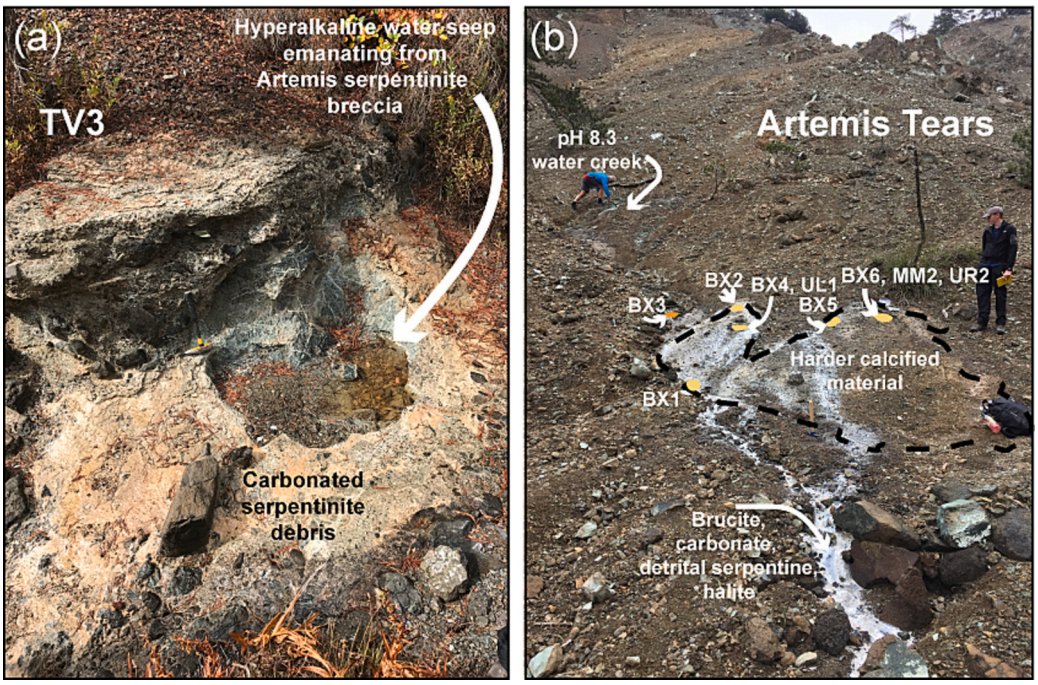

Fig. 4. (a) TV3 travertine deposit with pH 11.5 hyperalkaline water emanating from Artemis serpentinite breccia. Hammer for scale. (b) Artemis Tears with seep locations shown within area of harder calcified serpentinite material highlighted. White trails show detrital serpentinite loosely cemented by brucite-carbonate and halite precipitates resulting from mixing with pH 8.3 TMS waters.

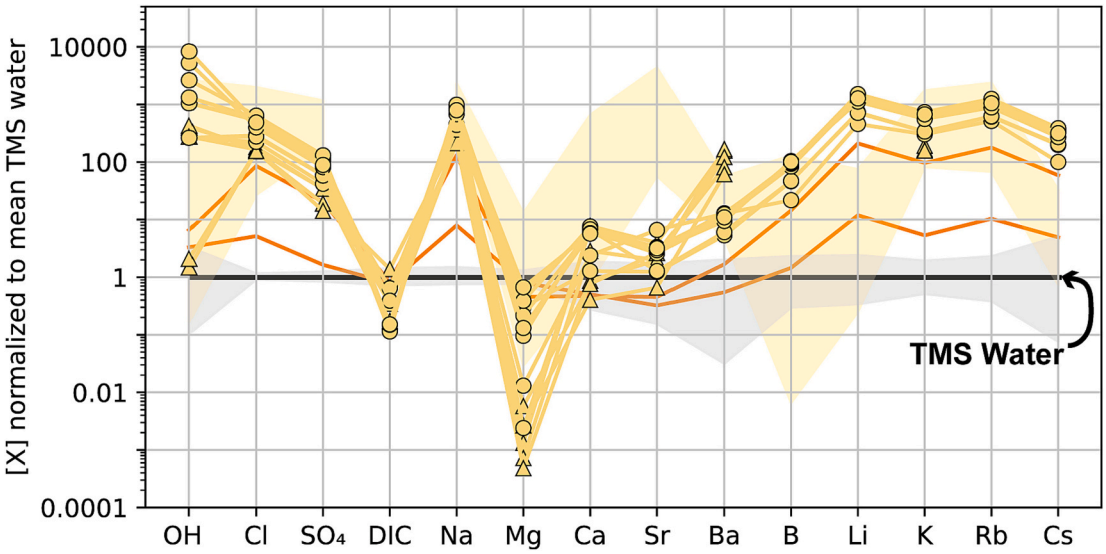

Fig. 5. Artemis Hyperalkaline water concentrations normalized to average TMS-waters (yellow circles), mixed waters (orange lines) from this study and the Alas spring (yellow triangles) (Rizoulis et al., 2016). Grey shading shows range of the TMS waters. Gold shading show Mariana Forearc serpentinite mud volcano fluids (Hulme et al., 2010; Mottl et al., 2004; Wheat et al., 2018).

fluids have $^{87}Sr/^{86}Sr$ ratios from 0.7079 to 0.7086, slightly displaced to less primitive values compared to TMS waters (Fig. 3a). Stable isotope analyses ($\delta^{18}O$ and δD) plot close to the Troodos meteoric water line (Fig. 3c).

4. Discussion

The Troodos Mantle surface waters (TMS waters) are similar to the Type 1 waters of Barnes and O'Neil (1969) and formed through near surficial reaction or meteoric waters with partly to completely serpentinized peridotites including primary (e.g., olivine, orthopyroxene) and secondary mineral (serpentine, brucite, carbonate) dissolution (Leong et al., 2021; Leong and Shock, 2020). Although these fluids are fresh (salinity <0.3 g/kg), relative to Cl, TMS waters have K-Rb-Cs as well as Li and B concentrations higher than seawater. This indicates the presence of a minor salt component that is not modern seawater aerosol. We note that snow from the Troodos massif does have the Na/Cl ratio of modern seawater (Table S1). Consequently, the enrichment in alkali metal ions and other components must be generated by fluid-rock interactions in addition to the dissolution of easy to mobilise solid phases such as brucite and carbonate. Stable isotope compositions of the TMS waters are close to the local meteoric water line indicating water

dominated fluid-rock exchanges as expected for near-surface groundwaters (Fig. 3). Sr concentrations are low and Sr-isotope compositions are between 0.7084 and 0.7086. This could point to exchange with ~20 million year old seawater, but is more likely to reflect dissolution of minor calcite veins with early Messinian seawater signatures ($^{87}Sr/^{86}Sr$ ~ 0.7086–9; Schildgen et al., 2014) mixed with a more primitive component.

In contrast, the Artemis hyperalkaline waters are some of the highest pH natural waters ever recorded (Fig. 2a; Monnin et al., 2014) and this signal is combined with high concentrations of dissolved salts. It is unusual that waters seeping from steep slopes of serpentinized gouge on a mountain comprising serpentinized peridotite have low Mg concentrations but high concentrations of alkali metals (Li, Na, K, Rb, Cs), B and Ba (Fig. 5), with Na/Cl ratios significantly elevated compared to seawater and potassium concentrations approaching that of modern seawater. High salinities combined with rock-equilibrated stable isotope compositions and rock-like $^{87}Sr/^{86}Sr$ ratios (Fig. 3) distinguishes the Artemis fluids from other hyperalkaline fluid suites, suggesting contributions from related but different fluid-rock reaction processes.

We suggest that the high pH values of the Artemis hyperalkaline waters are generated through multiple cycles of serpentine dissolution, recrystallisation and reprecipitation, following:

$$Mg_3Si_2O_5(OH)_4 + H_2O \rightleftharpoons 3Mg^{2+} + 2SiO_{2\ (aq)} + 6OH^-$$

Excess Mg^{2+} from this reaction has been extracted by precipitation of magnesite or brucite along the flow pathway (e.g., Leong et al., 2021; Leong and Shock, 2020), resulting in the observed anomalously low dissolved Mg and DIC (Fig. 5). Dissolved silica may precipitate as amorphous silica and/or contribute to the widespread occurrences of andradite in the sheared serpentine. Na/Cl ratios greater than seawater reflect additional Na^+ from dissolution of inclusions in the serpentine and this Na^+, plus other similarly dissolved cations, is balanced by the very high OH^- concentrations (Fig. 5).

The Amiantos mine waters are similar to the TMS waters but have higher dissolved salts suggesting either mixing with Artemis hyperalkaline waters or a process to enrich these waters in an additional component. Given the porous nature of the Amiantos tailings terraces and short flow paths for meteoric waters through these loose piles of waste rock, we favour the addition of a distinctive component.

All waters from the mantle sequences of the Troodos massif show elevated ratios of alkali metals (Li, K, Rb, Cs) and B over Cl compared to seawater, although these chemical enrichments are most apparent in the

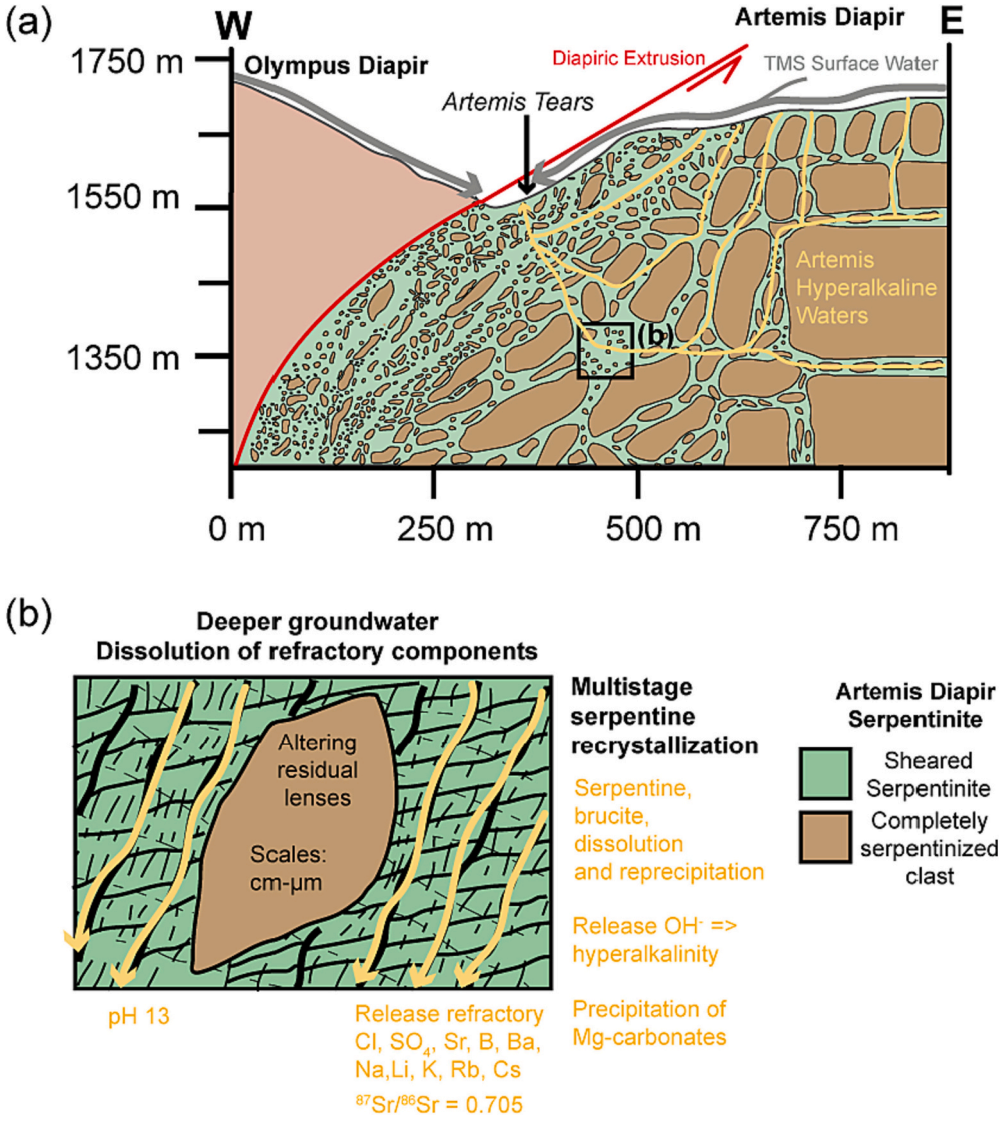

Fig. 6. (a) Cross section of the Artemis Tears site located near the boundary between the Olympus and Artemis diapirs. Fluid pathways for the TMS waters and hyperalkaline waters are shown. (b) inset schematic figure from (a) showing finer scale details resulting from dissolution of refractory components and occurrence of high pH 13 meteoric-derived hyperalkaline waters.

saline Artemis hyperalkaline waters. We suggest that both the partially serpentinized peridotites of the Olympus Diapir and the completely serpentinized peridotites of the Artemis Diapir include at least two serpentinization signatures; i) a loosely bound signature with low salinity and $^{87}Sr/^{86}Sr$ ratios of 0.7085 ± 0.0001 that can be mixed to different extents with ii) a strongly saline signature (elevated Cl, Na, K, Rb, Cs) with relatively primitive $^{87}Sr/^{86}Sr$ as well as high B, Li, Ba and sulfate. We propose that these strong saline signatures are sourced from inclusions of poorly soluble mineral(s), weakly bound to serpentine, within the serpentinized peridotites and have been mechanically advected by serpentine diapirism, uplift and erosion to the near surface environment where they are potentially available to be mobilised by groundwaters (Figs. 6,7). We are yet to identify the relatively refractory carrier phases of these saline and primitive ^{87}Sr signatures and these components are probably microscopic solid inclusions (e.g., Scambelluri et al., 2015, 1997), possibly entwinned within and protected by serpentine fibres rather than being directly bound in the serpentine structure. Some elements such as B may be accommodated within the crystalline serpentine structure (Pabst et al., 2011). It is only through the creation of new surface area through either tectonic deformation (Artemis Diapir) or crushing during mining operations that this relatively refractory phase becomes directly exposed to meteoric waters leading to elevated concentrations of these components in the groundwaters (Figs. 5,6).

4.1. Similarities and differences between Artemis hyperalkaline waters and Mariana serpentine seamount fluids

The Artemis hyperalkaline waters are substantially similar to saline high pH fluids issuing from serpentine seamounts in the Mariana forearc (e.g., Hulme et al., 2010; Mottl et al., 2004; Wheat et al., 2018) with similar pH, and Cl, SO_4, DIC, Na, Ca, Ba, B, K and Rb concentrations (Table 1, Fig. 2a; Fig. 5). The Mariana fluids have lower Mg, Li and Cs but much higher Sr concentrations. Notably the Mariana fluids have rock-like $^{87}Sr/^{86}Sr$ ratios (0.7054 to 0.7063; Bickford et al., 2008) and $\delta^{18}O$ ratios up to 4.4 ‰ (Benton, 1997) higher than modern seawater (Fig. 3c). Mixing between these high $\delta^{18}O$ Mariana ratios and TMS waters shows that the Artemis hyperalkaline waters are inconsistent with an origin of mixing between these two endmembers (Fig. 3c). Instead, the Artemis hyperalkaline waters are most consistent with strong exchange with serpentinites at low temperatures (<25 °C) (Fig. 3c).

Although the Mariana fluids are partially impacted by near ocean bottom fluid mixing processes and mineral precipitation reactions, the Mariana fluid compositions are interpreted to reflect hydrous fluid mobile inputs from the subducting slab beneath the serpentine mud volcanoes, with many tracers conservative and little affected by serpentinization reactions occurring in the overlying rigid mantle wedge (e.g., Mottl, 1992; Mottl et al., 2004). Fluid compositions vary with increasing distance from the Mariana trench and depth to and temperature of the underlying subducting slab, where conditions affect sediment and upper ocean crustal dehydration reactions, elemental mobilisation and extents of carbonate dissolution (Hulme et al., 2010; Menzies et al., 2022; Mottl et al., 2023, 2004; Wheat et al., 2020). Although the Marianas system is not directly analogous with the Troodos waters and we invoke different mechanical solid-phase mechanisms for the transport of slab signatures from depth to the surface, there are similarities particularly regarding the input of subduction zone signatures into mantle wedge serpentinites that are explored below (Fig. 5). The elevated Ca and Sr concentrations in the Marianas fluids farthest from the trench are proposed to reflect extensive carbonate dissolution from the lawsonite-epidote transition within the downgoing slab (e.g., Mottl et al., 2023, 2004). By comparison, the Artemis hyperalkaline waters yield relatively lower Ca and Sr concentrations indicating that the source zone of the Troodos subduction signatures is too cold for extensive carbonate dissolution (Fig. 5).

4.2. A geological model for the serpentinization of the Troodos Mantle Sequence and modern groundwaters

The >90 million year geological history of the Troodos ophiolite is complex and knowledge remains incomplete (e.g., Robertson, 1998). Even the current tectonic setting remains debated (e.g., Feld et al., 2017; Hall et al., 2005; Symeou et al., 2018; Welford et al., 2015). Following the formation of the Troodos crust at an east-west trending spreading ridge in a Neotethyan supra-subduction zone setting ~91 Ma (Mukasa and Ludden, 1987), the Troodos plate was rotated ~90° anticlockwise before the end of the lower Eocene during its accretion with the Mamonia terrane (Clube et al., 1985). Although there is evidence for Cretaceous near ridge serpentinization in peridotites of the Limassol Forest Complex along the Arakapas transform fault (e.g., Murton, 1986) (Fig. 1b) and during early uplift of those rocks prior to ~16 Ma (Robertson, 1977), there is little evidence for early serpentinization of the Troodos Mantle Sequence.

The modern subduction setting of Troodos is different from that which occurred in the Cretaceous (Robertson, 1998). Modern subduction was initiated approximately 20 million years ago (Robertson, 1998) in the Cyprean Trench about 50 km south of Cyprus. The plate being consumed is presumed to be Mesozoic or even Paleozoic ocean lithosphere (Feld et al., 2017; Granot, 2016; Müller et al., 2008; Welford et al., 2015) on the leading edge of the (relatively) northward-moving Sinai microplate ahead of the Eratosthenes plateau (Fig. 1a; Mascle et al., 2000) that is most likely submerged thinned continental crust.

Here we outline a sequence of events that best match the evidence for multiple serpentinization inputs including the strong subduction zone signature present in the Artemis hyperalkaline waters (Fig. 7). From the initiation of subduction until ~6 Ma, dewatering and dehydration reactions led to the pervasive but partial serpentinization of the overlying Cyprus mantle wedge and the addition of fluid mobile components to the subsurface peridotites that will be eventually exposed as the Olympus and Artemis domains (Fig. 7a). High concentrations of K, Rb and Cs and Na/Cl much greater than seawater indicate mobilisation of alkali metals from subducted ancient ocean crust (e.g., Mottl et al., 2004). Abundant Li may suggest a contribution from subducted sediments but the relatively primitive $^{87}Sr/^{86}Sr$ of this early serpentine signature indicates fluid inputs predominantly from altered ocean crust.

The collision of the Eratosthenes plateau with the Cyprean Trench about <5 Ma stalled the northwards subduction beneath Cyprus, leading to the focusing of fluids from the continued dehydration of the subducting plate to an east-west elongate region beneath the Troodos ophiolite with plate dewatering and dehydration and consequently fluid upwelling and serpentinization most concentrated beneath the present day Mount Olympus (Fig. 7b). This serpentinization of the mantle wedge led to the progressive uplift and emergence of the Troodos crust during the Messinian and the formation of small, isolated basins with irregular evaporite sequences (Manzi et al., 2016; Rouchy et al., 2001; Stow et al., 1995). Gabbroic rocks were first exposed in the Pliocene. The Troodos Mantle Sequence first became emergent in the earliest Pleistocene (McCallum, 1989; Poole and Robertson, 1998; Stow et al., 1995) (Fig. 7c) driven by continued serpentinization by slab dehydration fluids from below supplemented by the infiltration of rains falling on the rising topography of the nascent Troodos mountains leading to further uplift and erosion (Evans et al., 2021). Channelling of Messinian evaporite signatures including relatively radiogenic $^{87}Sr/^{86}Sr$ added an easily mobilised signature to the partially serpentinized Troodos peridotites (Fig. 7c).

Since the Late Pleistocene asbestiform serpentine has been present in the circum-Troodos sediments indicating the exposure of the completely altered serpentine blocks and highly deformed serpentine breccias and gouges of the Artemis Diapir (Fig. 7d, Evans et al., 2021). Primary geochemical evidence (Batanova and Sobolev, 2000) (Fig. 7d) indicates these rocks are from a distinctively different domain of the Cyprus mantle wedge.

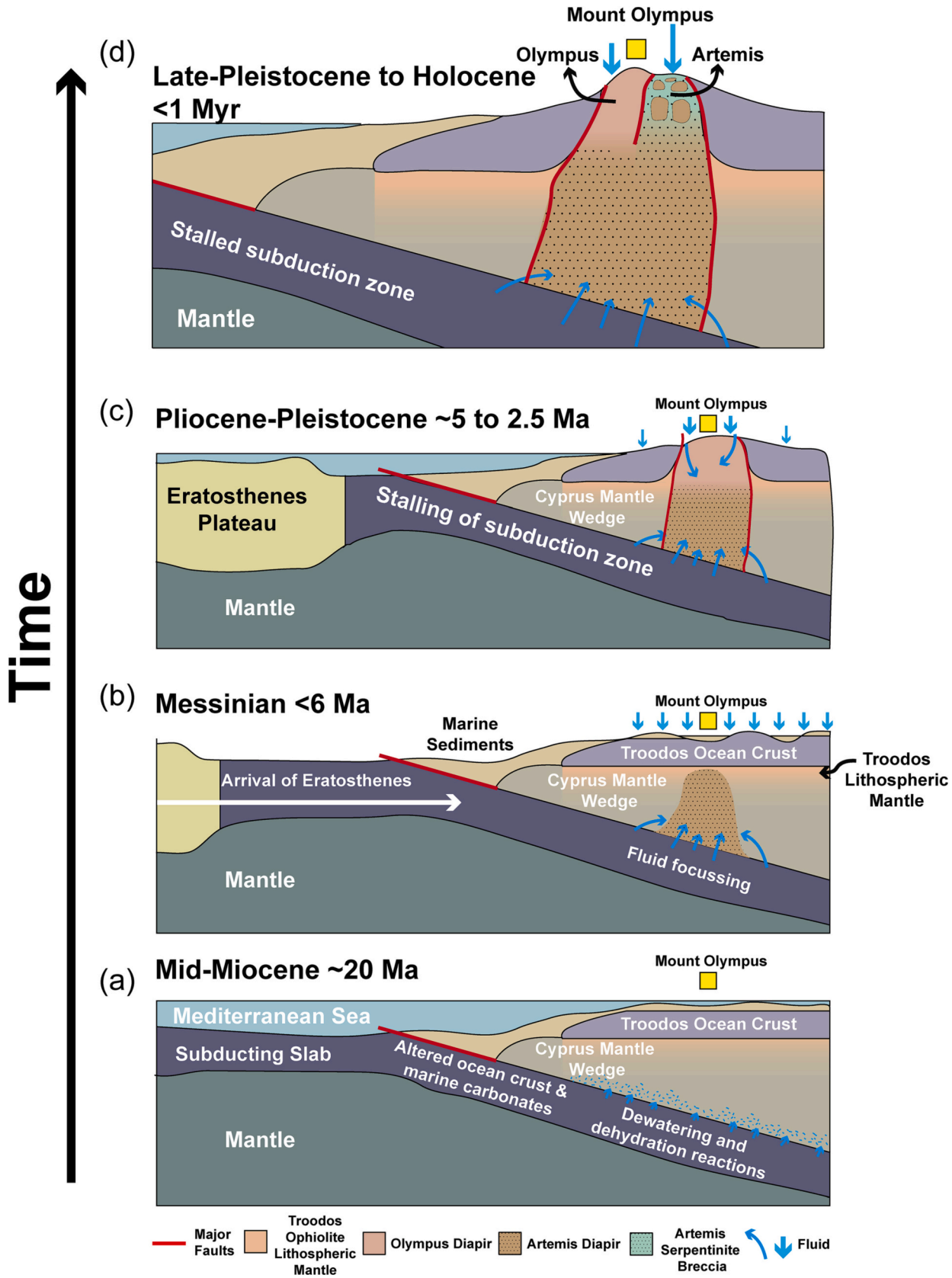

Fig. 7. Schematic figure of the Cyprus subduction zone show the progressive infusion of the Cyprus mantle wedge with subduction zone components (e.g., Li, Na, K, Rb, Cs) and its serpentinization from (a) Mid-Miocene, (b) Messinian, (c) Pliocene-Pleistocene, (d) Late-Pleistocene to Holocene. The progressive evolution of the subduction zone with the arrival of the incoming Eratosthenes Plateau that focussed slab-derived fluids beneath the Mount Olympus region, inducing serpentinite diapirism, and mechanically advecting signatures of subduction to the near-surface that are mobilised by meteoric waters. See text for details.

Modern rain and snow falling on the Troodos mantle sequences, form fresh, moderately alkaline Mg-HCO_3 "Type 1" fluids through the dissolution of serpentine, brucite and carbonate and acquire the distinctive $^{87}Sr/^{86}Sr$ signature of the Messinian evaporites. The deep subduction zone signatures likely remain tightly bound within the robust partially serpentinized peridotites of the Olympus Diapir. In contrast, some meteoric fluids penetrate more deeply into the breccias and highly deformed serpentinites of the Artemis Diapir, especially around the strongly brecciated boundary regions between the two domains. Through water-rock exchanges under highly rock-dominated conditions (Fig. 3c), these waters exchange stable isotopes and liberate relatively refractory subduction zone signatures from the strongly communited serpentine. These fluids emerge in rare, low flow rate springs. We note that the Artemis Tears site had not previously been recognised and was first identified following a winter of anomalously heavy rainfall (winter 2018/2019). This additional hydrological head may have pushed otherwise non-emergent deep hyperalkaline fluids to the surface. Although activity at the Artemis Tears site has continued (last observed May 2023) it has become progressively less active since first observed in 2019.

5. Conclusions

1) High pH (up to pH 13) hyperalkaline waters with very high salinities (25 to 30% seawater total dissolved loads) emanate in rare seeps within the Artemis Diapir of the Troodos massif, Cyprus. These fluids are unlike other high pH fluids that have been recorded in other ophiolite settings.
2) The Artemis hyperalkaline fluids most resemble waters from the Mariana forearc serpentinite seamounts with elevated concentrations of alkali elements (Li, Na, K, Rb, Cs), B and Ba. Despite the similarities of these hyperalkaline fluids, the Artemis hyperalkaline waters show evidence of extensive exchange between meteoric water and the completely serpentinized mantle rocks of the Artemis Diapir.
3) We propose that the stalling of Cyprus subducting plate has led to the widespread infusion of the Cyprus mantle wedge with subduction zone signatures (Li, Na, K, Rb, Cs) $^{87}Sr/^{86}Sr$, B and Ba, held in relatively refractory phases. Serpentine diapirism has led to the uplift and exposure of the Troodos Mantle Sequence. Localized deformation in the Artemis Diapir and multiple cycles of serpentine recrystallization and reprecipitation has allowed deeply penetrating meteoric waters to mobilise these subduction zones signatures that emerge in rare high pH (11 to 13) saline waters with low $^{87}Sr/^{86}Sr$ and rock-dominated stable isotope compositions.
4) Although all fluids draining the Troodos Mantle Sequence show elevated fluid mobile element/Cl ratios relative to seawater, Amiantos mine waters show elevated concentrations (relative to TMS waters) in fluid mobile elements made available by industrial comminution.

Declaration of Competing Interest

The authors declare that they have no known competing financial interests or personal relationships that could have appeared to influence the work reported in this paper.

Data availability

All data used in this study are provided in the supplementary materials or are cited accordingly.

Acknowledgements

We thank the Geological Survey Department of the Republic of Cyprus for facilitating field work and particularly Christos Christofi for discussions on groundwater chemistry in the Troodos crust and for sharing his PhD thesis (MoU/Ref. No. 05.26.001/5). Aled D. Evans acknowledges a Natural Environment Research Council-SPITFIRE CASE PhD award NE/L002531/1 (Natural History Museum CASE Partner) and a Natural Environment Research Council-NIGFSC IP-1833-0618 awarded to ADE and DAHT. DAHT acknowledges a Royal Society Wolfson Research Merit Award (WM130051). Adrian Boyce is thanked for facilitating oxygen and hydrogen stable isotope analyses at the Scottish Universities Environmental Research Centre (SUERC; IP-1833-0618). Rachael H. James, Juerg M. Matter, M. Grace Andrews, Catriona D. Menzies, are thanked for conversations on water sampling methods and hyperalkaline waters. Aspects of this study were refined whilst DAHT was kindly hosted as a sabbatical visitor at Nga ara whetu/Centre for Climate, Biodiversity and Society, University of Auckland. We thank Michael Böttcher for editorial handling, and Gretchen Früh-Green and Jeff Alt for their constructive reviews.

Appendix A. Supplementary data

Supplementary data to this article can be found online at https://doi.org/10.1016/j.chemgeo.2023.121822.

Reference list

Alt, J.C., 1994. A sulfur isotopic profile through the troodos ophiolite, Cyprus: primary composition and the effects of seawater hydrothermal alteration. Geochim. Cosmochim. Acta 58, 1825–1840.
Barnes, I., O'Neil, J.R., 1969. The relationship between fluids in some fresh alpine-type ultramafics and possible modern serpentinization, Western United States. GSA Bull. 80, 1947–1960.
Barnes, I., Lamarche, V.C., Himmelberg, G., 1967. Geochemical evidence of present-day serpentinization. Science 156, 830–832.
Barnes, I., O'Neil, J.R., Trescases, J.J., 1978. Present day serpentinization in New Caledonia, Oman and Yugoslavia. Geochim. Cosmochim. Acta 42, 144–145.
Batanova, V.G., Sobolev, A.V., 2000. Compositional heterogeneity in subduction-related mantle peridotites, Troodos massif, Cyprus. Geology 28, 55.
Benton, L.D., 1997. Origin and Evolution of Serpentine Seamount Fluids, Mariana and Izu-Bonin Forearcs: Implications for the Recycling of Subducted Material. Ph.D. The University of Tulsa, Ann Arbor, United States.
Bickford, M.E., Siegel, D.I., Mottl, M.J., Hill, B.M., Shosa, J., 2008. Strontium isotopic relations among pore fluids, serpentine matrix, and harzburgite clasts, South Chamorro Seamount, Mariana forearc. Chem. Geol. 256, 24–32.
Boronina, A., Renard, P., Balderer, W., Christodoulides, A., 2003. Groundwater resources in the Kouris catchment (Cyprus): data analysis and numerical modelling. J. Hydrol. 271, 130–149.
Boronina, A., Balderer, W., Renard, P., Stichler, W., 2005a. Study of stable isotopes in the Kouris catchment (Cyprus) for the description of the regional groundwater flow. J. Hydrol. 308, 214–226.
Boronina, A., Golubev, S., Balderer, W., 2005b. Estimation of actual evapotranspiration from an alluvial aquifer of the Kouris catchment (Cyprus) using continuous streamflow records. Hydrol. Process. 19, 4055–4068.
Boschetti, T., Etiope, G., Pennisi, M., Romain, M., Toscani, L., 2013. Boron, lithium and methane isotope composition of hyperalkaline waters (Northern Apennines, Italy): terrestrial serpentinization or mixing with brine? Appl. Geochem. 32, 17–25.
Chavagnac, V., Monnin, C., Ceuleneer, G., Boulart, C., Hoareau, G., 2013. Characterization of hyperalkaline fluids produced by low-temperature serpentinization of mantle peridotites in the Oman and Ligurian ophiolites. Geochem. Geophys. Geosyst. 14, 2496–2522.
Christofi, C., 2020. The Hydrogeochemical Regime of the Troodos Fractured Aquifer: A Comprehensive Approacnh. Ph.D.. The Cyprus Institute.
Christofi, C., Bruggeman, A., Kuells, C., Constantinou, C., 2020a. Isotope hydrology and hydrogeochemical modeling of Troodos Fractured Aquifer, Cyprus: the development of hydrogeological descriptions of observed water types. Appl. Geochem. 123, 104780.
Christofi, C., Bruggeman, A., Kuells, C., Constantinou, C., 2020b. Hydrochemical evolution of groundwater in gabbro of the Troodos fractured aquifer. A comprehensive approach. Appl. Geochem. 114, 104524.
Clube, T.M.M., Creer, K.M., Robertson, A.H.F., 1985. Palaeorotation of the Troodos microplate, Cyprus. Nature 317, 522–525.
Evans, A.D., Teagle, D.A.H., Craw, D., Henstock, T.J., Falcon-Suarez, I.H., 2021. Uplift and exposure of serpentinized massifs: Modeling differential serpentinite diapirism and exhumation of the troodos mantle sequence, Cyprus. J. Geophys. Res. Solid Earth 126. https://doi.org/10.1029/2020jb021079.
Feld, C., Mechie, J., Hübscher, C., Hall, J., Nicolaides, S., Gurbuz, C., Bauer, K., Louden, K., Weber, M., 2017. Crustal structure of the Eratosthenes Seamount, Cyprus and S. Turkey from an amphibian wide-angle seismic profile. Tectonophysics 700–701, 32–59.
Gass, I.G., Masson-Smith, D., 1963. The geology and gravity anomalies of the Troodos Massif, Cyprus. Proc. R. Soc. B Biol. Sci. 157, 587–588.

Gat, J.R., Mazor, E., Tzur, Y., 1969. The stable isotope composition of mineral waters in the Jordan Rift Valley, Israel. J. Hydrol. 7, 334–352.
Georgiou, A., 2002. Assessment of Groundwater Resources of Cyprus; Reassessment of the island's water resources and demand-Objective 1–output 1.4.2. Water Development Department—Ministry of Agriculture, Rural Development and Environment, Nicosia, Cyprus, p. 234.
Giampouras, M., Garrido, C.J., Zwicker, J., Vadillo, I., Smrzka, D., Bach, W., Peckmann, J., Jiménez, P., Benavente, J., García-Ruiz, J.M., 2019. Geochemistry and mineralogy of serpentinization-driven hyperalkaline springs in the Ronda peridotites. Lithos 350–351, 105215.
Granot, R., 2016. Palaeozoic oceanic crust preserved beneath the eastern Mediterranean. Nat. Geosci. 9, 701–705.
Hall, J., Calon, T.J., Aksu, A.E., Meade, S.R., 2005. Structural evolution of the Latakia Ridge and Cyprus Basin at the front of the Cyprus Arc, Eastern Mediterranean Sea. Mar. Geol. 221, 261–297.
Herzig, P.M., Friedrich, G.H., 1987. Sulphide mineralization, hydrothermal alteration and chemistry in the drill hole CY-2a, Agrokipia, Cyprus. In: Robinson, P.T., Gibson, I.L., Panayioutou, A. (Eds.), Cyprus Crustal Study Project, Holes CY2 and 2a, Geol Surv. Can. Pap. 85-29., pp. 103–138.
Hulme, S.M., Wheat, C.G., Fryer, P., Mottl, M.J., 2010. Pore water chemistry of the Mariana serpentinite mud volcanoes: a window to the seismogenic zone. Geochem. Geophys. Geosyst. 11 https://doi.org/10.1029/2009gc002674.
Jamieson, H.E., Lyndon, J.A., 1987. Geochemistry of a fossil ore solution aquifer: Chemical exchange between rock and hydrothermal fluid recorded in the lower portion of research Drill Hole CY-2a, Agrokipia, Cyprus. In: Robinson, P.T., Gibson, I. L., Panayioutou, A. (Eds.), Cyprus Crustal Study Project, Holes CY2 and 2a. Geol. Surv. Can. Pap. 85-29, pp. 139–152.
Kelemen, P.B., Matter, J., 2008. In situ carbonation of peridotite for CO_2 storage. Proc. Natl. Acad. Sci. 105, 17295–17300.
Kelemen, P.B., Matter, J., Streit, E.E., Rudge, J.F., Curry, W.B., Blusztajn, J., 2011. Rates and Mechanisms of Mineral Carbonation in Peridotite: Natural Processes and Recipes for Enhanced, in situ CO_2 Capture and Storage. Annu. Rev. Earth Planet. Sci. 39, 545–576.
Kelley, D.S., Karson, J.A., Blackman, D.K., Früh-Green, G.L., Butterfield, D.A., Lilley, M. D., Olson, E.J., Schrenk, M.O., Roe, K.K., Lebon, G.T., Rivizzigno, P., Party, T.A., 2001. An off-axis hydrothermal vent field near the Mid-Atlantic Ridge at 30° N. Nature 412, 145–149.
Kerrick, D., 2002. Geology. Serpentinite seduction. Science 298, 1344–1345.
Leong, J.A.M., Shock, E.L., 2020. Thermodynamic constraints on the geochemistry of low-temperature, continental, serpentinization-generated fluids. Am. J. Sci. 320, 185–235.
Leong, J.A.M., Howells, A.E., Robinson, K.J., Cox, A., Debes II, R.V., Fecteau, K., Prapaipong, P., Shock, E.L., 2021. Theoretical predictions versus environmental observations on serpentinization fluids: lessons from the Samail ophiolite in Oman. J. Geophys. Res. Solid Earth 126. https://doi.org/10.1029/2020jb020756.
Manzi, V., Lugli, S., Roveri, M., Dela Pierre, F., Gennari, R., Lozar, F., Natalicchio, M., Schreiber, B.C., Taviani, M., Turco, E., 2016. The Messinian salinity crisis in Cyprus: a further step towards a new stratigraphic framework for Eastern Mediterranean. Basin Res. 28, 207–236.
Mascle, J., Prismed II Scientific Party, Benkhelil, J., Bellaiche, G., Zitter, T., Woodside, J., Loncke, L., 2000. Marine geologic evidence for a Levantine-Sinai plate, a new piece of the Mediterranean puzzle. Geology 28, 779–782.
McArthur, J.M., Howarth, R.J., Shields, G.A., 2012. Strontium Isotope Stratigraphy. In: The Geologic Time Scale. Elsevier, pp. 127–144.
McCallum, J.E., 1989. Sedimentation and Tectonics of the Plio-Pleistocene of Cyprus. Ph. D.. University of Edinburgh.
Mederer, J., 2009. Water Resources and Dynamics of the Troodos Igneous Aquifer-System, Cyprus - Balanced Groundwater Modelling. Ph.D.. Universität Würzburg.
Menzies, C.D., Price, R.E., Ryan, J., Sissmann, O., Takai, K., Wheat, C.G., 2022. Spatial variation of subduction zone fluids during progressive subduction: Insights from Serpentinite Mud Volcanoes. Geochim. Cosmochim. Acta 319, 118–134.
Monnin, C., Chavagnac, V., Boulart, C., Ménez, B., Gérard, M., Gérard, E., Pisapia, C., Quéméneur, M., Erauso, G., Postec, A., Guentas-Dombrowski, L., Payri, C., Pelletier, B., 2014. Fluid chemistry of the low temperature hyperalkaline hydrothermal system of Prony Bay (New Caledonia). Biogeosciences 11, 5687–5706.
Moores, E.M., Vine, F.J., 1971. The Troodos Massif, Cyprus and other ophiolites as Oceanic crust: evaluation and implications. Philos. Trans. R. Soc. A Math. Phys. Eng. Sci. 268, 443–467.
Moores, E.M., Robinson, P.T., Malpas, J., Xenophonotos, C., 1984. Model for the origin of the Troodos massif, Cyprus, and other mideast ophiolites. Geology 12, 500–503.
Morag, N., Haviv, I., Katzir, Y., 2016. From ocean depths to mountain tops: Uplift of the Troodos ophiolite (Cyprus) constrained by low-temperature thermochronology and geomorphic analysis. Tectonics 35, 622–637.
Mottl, M.J., 1992. Pore Waters from Serpentinite Seamounts in the Mariana and Izu-Bonin Forearcs, Leg 125: evidence for Volatiles from the Subducting Slab. In: Proceedings of the Ocean Drilling Program, 125 Scientific Results. Ocean Drilling Program, pp. 373–385.
Mottl, M.J., Wheat, C.G., Fryer, P., Gharib, J., Martin, J.B., 2004. Chemistry of springs across the Mariana forearc shows progressive devolatilization of the subducting plate. Geochim. Cosmochim. Acta 68, 4915–4933.
Mottl, M.J., McCollom, T.M., Wheat, C.G., Fryer, P., 2023. Chemistry of springs across the Mariana forearc: carbon flux from the subducting plate triggered by the lawsonite-to-epidote transition? Geochim. Cosmochim. Acta 340, 1–20.
Mukasa, S.B., Ludden, J.N., 1987. Uranium-lead isotopic ages of plagiogranites from the Troodos ophiolite, Cyprus, and their tectonic significance. Geology 15, 825.
Müller, R.D., Sdrolias, M., Gaina, C., Roest, W.R., 2008. Age, spreading rates, and spreading asymmetry of the world's ocean crust. Geochem. Geophys. Geosyst. 9 https://doi.org/10.1029/2007gc001743.
Murton, B.J., 1986. Anomalous oceanic lithosphere formed in a leaky transform fault: evidence from the Western Limassol Forest complex, Cyprus. J. Geol. Soc. Lond. 143, 845–854.
Neal, C., Shand, P., 2002. Spring and surface water quality of the Cyprus ophiolites. Hydrol. Earth Syst. Sci. 6, 797–817.
Neal, C., Stanger, G., 1985. Past and present serpentinisation of ultramafic rocks, an example from the Semail Ophiolite Nappe of Northern Oman. In: The Chemistry of Weathering. Springer, Netherlands, Dordrecht, pp. 249–275.
Pabst, S., Zack, T., Savov, I.P., Ludwig, T., Rost, D., Vicenzi, E.P., 2011. Evidence for boron incorporation into the serpentine crystal structure. Am. Mineral. 96, 1112–1119.
Pearce, J.A., Lippard, S.J., Roberts, S., 1984. Characteristics and Tectonic Significance of Supra-Subduction Zone Ophiolites. Geological Society, London.
Poole, A., Robertson, A., 1998. Pleistocene fanglomerate deposition related to uplift of the Troodos Ophiolite, Cyprus. In: Robertson, A.H.F., Emeis, K.-C., Richter, C., Camerlenghi, A. (Eds.), Proc. ODP, Sci. Results, Vol. 160. Ocean Drilling Program, College Station, TX, pp. 545–566.
Poole, A.J., Robertson, A.H.F., 1991. Quaternary uplift and sea-level change at an active plate boundary, Cyprus. J. Geol. Soc. Lond. 148, 909–921.
Rautenschlein, M., Jenner, G.A., Hertogen, J., Hofmann, A.W., Kerrich, R., Schmincke, H. U., White, W.M., 1985. Isotopic and trace element composition of volcanic glasses from the Akaki Canyon, Cyprus: implications for the origin of the Troodos ophiolite. Earth Planet. Sci. Lett. 75, 369–383.
Rizoulis, A., Milodowski, A.E., Morris, K., Lloyd, J.R., 2016. Bacterial diversity in the hyperalkaline allas springs (Cyprus), a natural analogue for cementitious radioactive waste repository. Geomicrobiol J. 33, 73–84.
Robertson, A.H.F., 1977. Tertiary uplift history of the Troodos massif, Cyprus. GSA Bull. 88, 1763–1772.
Robertson, A.H.F., 1998. Mesozoic-Tertiary tectonic evolution of the easternmost Mediterranean area: integration of marine and land evidence. Proc. Ocean Drill. Program Sci. Results 723–782.
Rouchy, J.M., Orszag-Sperber, F., Blanc-Valleron, M.-M., Pierre, C., Rivière, M., Combourieu-Nebout, N., Panayides, I., 2001. Paleoenvironmental changes at the Messinian–Pliocene boundary in the eastern Mediterranean (southern Cyprus basins): significance of the Messinian Lago-Mare. Sediment. Geol. 145, 93–117.
Saad, A.H., 1969. Magnetic properties of ultramafic rocks from Red Mountain, California. Geophysics 34, 974–987.
Saccocia, P.J., Seewald, J.S., Shanks III, W.C., 2009. Oxygen and hydrogen isotope fractionation in serpentine–water and talc–water systems from 250 to 450 C, 50 MPa. Geochim. Cosmochim. Acta 73, 6789–6804.
Scambelluri, M., Piccardo, G.B., Philippot, P., Robbiano, A., Negretti, L., 1997. High salinity fluid inclusions formed from recycled seawater in deeply subducted alpine serpentinite. Earth Planet. Sci. Lett. 148, 485–499.
Scambelluri, M., Pettke, T., Cannaò, E., 2015. Fluid-related inclusions in Alpine high-pressure peridotite reveal trace element recycling during subduction-zone dehydration of serpentinized mantle (Cima di Gagnone, Swiss Alps). Earth Planet. Sci. Lett. 429, 45–59.
Schildgen, T.F., Cosentino, D., Frijia, G., Castorina, F., Dudas, F.Ö., Iadanza, A., Sampalmieri, G., Cipollari, P., Caruso, A., Bowring, S.A., Strecker, M.R., 2014. Sea level and climate forcing of the Sr isotope composition of late Miocene Mediterranean marine basins. Geochem. Geophys. Geosyst. 15, 2964–2983.
Shelton, A.W., 1993. Troodos revisited: the Mount Olympus gravity anomaly. Geol. Soc. Lond. Spec. Publ. 76, 197–212.
Stow, D.A.V., Braakenburg, N.E., Xenophontos, C., 1995. The Pissouri Basin fan-delta complex, southwestern Cyprus. Sediment. Geol. 98, 245–262.
Symeou, V., Homberg, C., Nader, F.H., Darnault, R., Lecomte, J.-C., Papadimitriou, N., 2018. Longitudinal and temporal evolution of the tectonic style along the Cyprus arc system, assessed through 2-D reflection seismic interpretation. Tectonics 37, 30–47.
Taylor, H.P., 1977. Water/rock interactions and the origin of H2O in granitic batholiths: Thirtieth William Smith lecture. J. Geol. Soc. Lond. 133, 509–558.
Welford, J.K., Hall, J., Hübscher, C., Reiche, S., Louden, K., 2015. Crustal seismic velocity structure from Eratosthenes Seamount to Hecataeus rise across the Cyprus Arc, eastern Mediterranean. Geophys. J. Int. 200, 935–953.
Wenner, D.B., Taylor, H.P., 1971. Temperatures of serpentinization of ultramafic rocks based on O18/O16 fractionation between coexisting serpentine and magnetite. Contrib. Mineral. Petrol. 32, 165–185.
Wheat, C.G., Fournier, T., Paul, C., Menzies, C., Price, R.E., Ryan, J., Sissman, O., 2018. Data Report: IODP Expedition 366 Pore Water Trace Element (V, Mo, Rb, Cs, U, Ba, and Li) Compositions. School Geosci. Faculty Staff Public. 366 https://doi.org/10.14379/iodp.proc.366.201.2018.
Wheat, C.G., Seewald, J.S., Takai, K., 2020. Fluid transport and reaction processes within a serpentinite mud volcano: South Chamorro Seamount. Geochim. Cosmochim. Acta 269, 413–428.
Wilson, R.A.M., 1959. The Geology of the Xeros-Troodos Area (No. 1). Authority of the Government of Cyprus.